

Smart windows passively driven by greenhouse effect

G. Boudan,^{1,2} E. Eustache,² P. Garabedian,² R. Messina,¹ and P. Ben-Abdallah^{1,*}

¹Laboratoire Charles Fabry, UMR 8501, Institut d'Optique, CNRS,

Université Paris-Saclay, 2 Avenue Augustin Fresnel, 91127 Palaiseau Cedex, France.

²Thales Research and Technology France, 1, Avenue Augustin Fresnel, F-91767 Palaiseau, Cedex France.

(Dated: October 14, 2022)

The rational thermal management of buildings is of major importance for the reduction of the overall primary energy consumption. Smart windows are promising systems which could save a significant part of this energy. Here we introduce a double glazing system made with a thermochromic metal-insulator transition material and a glass layer separated by an air gap which is able to switch from its insulating to its conducting phase thanks to the greenhouse effect occurring in the separation gap. We show that this passive system can reduce the incoming heat flux by more than 40% in comparison with traditional windows while maintaining the transmittance in the visible range at a relatively high level.

Nowadays buildings consume about 40% of the primary energy used in the world [1]. Therefore their thermal management is a major concern in the context of current global challenge of energy efficiency. Smart windows could play a major role to respond to this challenge. These windows can be used to control heat flux exchanged between the indoor and external environment. One way to achieve this control is by tuning the radiative properties of these systems. Hence, by controlling the overall emissivity/transmittivity of a window surface it is possible to facilitate or reduce heat exchange with the environment and therefore to act directly on the indoor temperature. Several strategies have been proposed so far to perform such a control. For example, single glazings made of thermochromic materials have been suggested [2–4] to tailor the optical properties of windows with respect to their temperature. Among these materials vanadium dioxide (VO_2) a metal-insulator transition (MIT) material has been largely investigated. Due to their pronounced change of optical properties in the infrared these phase-change materials have found numerous applications in the fields of thermal management [5–9], energy storage [10] and information treatment [11]. However this material undergoes a reversible structural phase transition at relatively high temperature ($T_C \sim 68^\circ\text{C}$) making its employment challenging in smart windows. Moreover, to date, there is no real alternative candidate to this material presenting a pronounced MIT close to the ambient temperature. Electrochromic materials have also been proposed [12, 13] to modify the optical properties of smart windows using an external bias voltage. Hence, by using VO_2 solid-electrolyte films, the light transmittance of such gate-controlled smart windows can be dramatically modified by tuning the hydrogen-ion doping through gating voltage. However, although this optical control can operate at ambient temperature it requires an external energy supply. Moreover, electrochromic windows are mainly effective in blocking visible light and not infrared radiation so that their thermal performances remain today

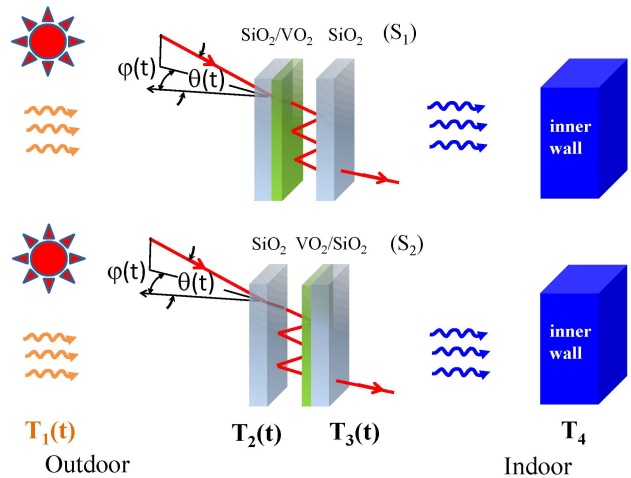


Figure 1: Sketch of the passive smart window made with a double glazing of two SiO_2 layers separated by an air gap and a VO_2 thin film deposited on the inner side of one of the two glass panes. The crystalline phase of the VO_2 layer is driven by the greenhouse effect occurring between the two panes thanks to the external sunshine in the visible range and by the heat flux radiated in the infrared by the surrounding environment and the inner wall.

very weak.

In the present letter we introduce a passive smart window based on a double glazing system (Fig.1) realized with a VO_2 film deposited on the internal side of the glazing. The two panes of this glazing are separated by few-millimeters thick air gap. Following the evolution during the day of external conditions of sunshine evolve during the day the temperature of this MIT material changes thanks to the greenhouse effect occurring between the two panes. By optimizing the geometry of this system we show that we can at the same time control its transmittance in the visible range and the incoming heat flux. More specifically, by analyzing the temporal evolution of this thermo-optical system driven by the external sunshine and the heat flux radiated in the in-

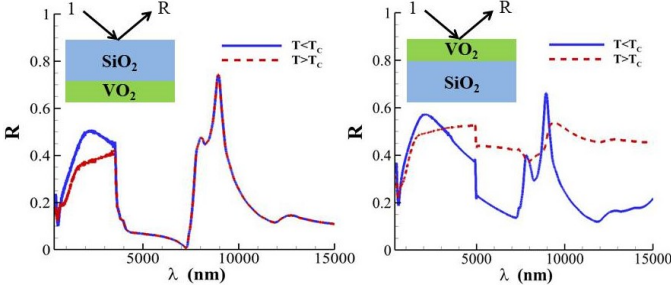


Figure 2: Reflectance spectra (averaged over the two polarization states) of $SiO_2 - VO_2$ (left) and $VO_2 - SiO_2$ (right) bilayer across the MIT process. The glass layer is 5 mm thick while the thickness of VO_2 film is 100 nm .

framed by the external environment and the inner walls we show that our smart-window design results in a significant reduction of the heat flux reaching the inner side, compared to traditional windows, in conjunction with a low reduction of the transmittance in the visible range of the spectrum.

To start let us describe the physical characteristics of system. The active part is made of a vanadium dioxide (VO_2) film which undergoes a first-order transition (Mott transition [14]) from a high-temperature metallic phase to a low-temperature insulating phase [15, 16] at T_C . This film is deposited on a glass layer which is partially transparent in the infrared range [17]. As a result of the phase transition both the emissivity and the reflectivity of this bilayer change radically (Fig.2) on its two sides both in the visible and in the infrared. The outside pane of the window is assumed to be in contact with a thermal bath having temperature $T_1(t)$ and is illuminated by the sun with a time-varying flux $\Phi_2(t)$ depending on the sun trajectory during the day. For the sake of simplicity, the field radiated by the bath can be assimilated to the field radiated by a blackbody at the same temperature. On its opposite side the window interacts with the inner walls of average emissivity ϵ at temperature T_4 . Due to the thermal inertia of walls, T_4 is assumed here constant during a solar cycle.

The optical properties (emissivity/transmittivity) of the window are driven by the temperature of each pane and therefore by the heat flux they exchange between them and with the outdoor and indoor environments. The time evolution of the thermal state ($T_2(t), T_3(t)$) of the window under the external driving is governed by the coupled energy-balance equations

$$C_i \frac{dT_i}{dt} = \sum_{j \neq i} \mathcal{P}_{j \rightarrow i}(T_1, \dots, T_4; t) + \Phi_i(t), \quad i = 2, 3. \quad (1)$$

Here $\mathcal{P}_{j \rightarrow i}$ denotes the surfacic power received by the i^{th} element from the j^{th} element within the system, Φ_i the contribution of solar flux and C_i the heat capacity per unit surface for the pane i of the window. Generally

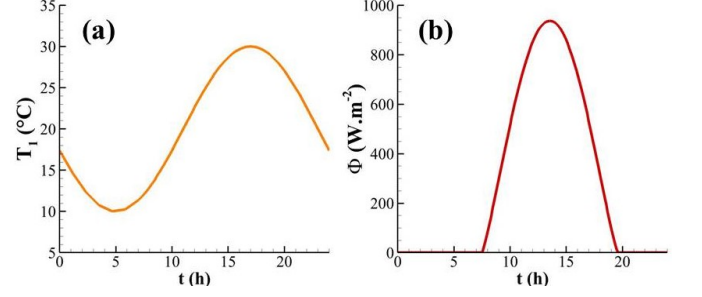


Figure 3: Time evolution during a typical summer day of the external temperature (a) and that of solar flux (b) at a latitude of 48.2° .

speaking these powers can be expressed into a Landauer-like form [18, 19]

$$\mathcal{P}_{j \rightarrow i}(t) = \int_0^\infty \frac{d\omega}{2\pi} [\Theta(\omega, T_j(t)) - \Theta(\omega, T_i(t))] \times \sum_{l=(s,p)} \int_{\kappa < \omega/c} \frac{d\kappa}{2\pi} \kappa \mathcal{T}_l^{ji}(\omega, \kappa), \quad (2)$$

where $\mathcal{T}_l^{ji}(\omega, \kappa)$ denotes the transmission coefficient (the detailed expressions are given in Ref. [19] with respect to the reflectivity, transmittivity and emissivity of each element) for each electromagnetic mode (ω, κ) (ω being the mode pulsation and κ the component of wavenumber parallel to the window surface) and each polarization ($s = TE, p = TM$) between the two elements at temperature T_j and T_i while $\Theta(\omega, T) = \frac{\hbar\omega}{e^{\frac{\hbar\omega}{k_B T}} - 1}$ is the mean energy of a harmonic oscillator at temperature T . In expression Eq.(2) the summation is made over the propagative modes (i.e. $\kappa < \omega/c$) all separation distances between the different parts of system being much larger than the modes' wavelength. The transmission coefficient can be expressed [19] in term of the reflection operators of each part of the system. The solar flux plotted in Fig. 3(b) is calculated from the AM1.5 Global spectrum [20] over a daily cycle for a window facing south. We also assume a sinusoidal variation of the outdoor temperature [Fig.3-(a)] with a minimal value $T_1^{\text{min}} = 10^\circ\text{ C}$ at 5 a.m. and a maximal value $T_1^{\text{max}} = 30^\circ\text{ C}$ at 4 p.m. , corresponding to a typical variation of this temperature during summer. Finally, in order to demonstrate the operating mode of the window we assume the inner wall perfectly absorbing (i.e. $\epsilon = 1$). The time evolution of these two primary sources being very slow in comparison with the thermalization time of glazing (\sim few seconds to the minute), the energy balance Eq. (1) can be solved in the adiabatic approximation.

The solutions ($T_2(t), T_3(t)$) of this balance equation corresponding to the external conditions (solar flux $\Phi(t)$, outdoor temperatures $T_1(t)$) given the indoor temperature $T_4 = 25^\circ\text{ C}$ are plotted in Fig.4 for different thicknesses of VO_2 film and compared to the thermal state of a

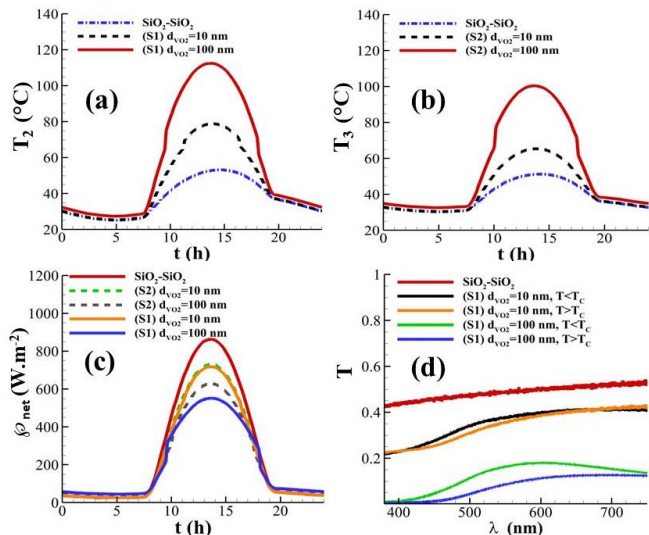


Figure 4: Thermal state and performances of the smart window. (a) Evolution of panes temperature in a S_1 -type window. (b) Temperatures in a window of S_2 -type. (c) Incoming net power \mathcal{P}_{net} with respect to time for a S_1 and S_2 window and its comparison with a traditional double glazing. The glass and VO_2 films have thicknesses $d_{SiO_2} = 5$ mm and $d_{VO_2} = 10$ nm or $d_{VO_2} = 100$ nm, respectively. (d) Transmittance in the visible range of the smart window (S_1 configuration) below (resp. beyond) the critical temperature T_C and its comparison with a double glazing SiO_2 - SiO_2 .

simple glass-glass double glazing. As shown in Figs.4(a) and (b) the temperature of the active layer can reach, at the midday, levels significantly higher than the critical temperature T_C . The comparison of T_1 (resp. T_2) with the temperatures of a double (glass-glass) glazing of same thickness demonstrates the presence of a strong greenhouse effect in the designed window due to the trapping of the infrared light in the separation gap between the two panes. The magnitude of this effect is directly related to the thickness of VO_2 film. As shown in Figs.4(a) and (b), the thicker is this film the greater is the blocked infrared radiation in the separation gap between the two panes of glazing. The heating induced by this greenhouse effect in the smart window surpasses the one traditionally observed in the traditional double-glazing window by more than 100% with VO_2 film 100 nm thick in S_1 -type configuration and it is still 100% higher with a film 10 nm in the same configuration. The physical consequences of this heating are shown in Figs.4(c) and (d) demonstrating both the thermal and optical performances of this smart window. The net incoming heat flux, with respect to time, plotted in Fig.4(c)

$$\mathcal{P}_{net}(t) = \Phi_4(t) + \sum_{j \neq 4} \mathcal{P}_{j \rightarrow 4}(t) - \sum_{j \neq 3} \mathcal{P}_{3 \rightarrow j}(t) \quad (3)$$

is drastically reduced in comparison with a traditional window (double glazing SiO_2 - SiO_2). This reduction is

approximately $325 W \cdot m^{-2}$ at the midday when the VO_2 film $d_{VO_2} = 100$ nm is deposited on the inner side of the external pane (S_1 configuration in Fig.1), a value representing 33% of the solar irradiation at 48.2° latitude and about 40% of the incoming flux through a traditional window. Such isolating behavior exceeds by far the performances of all previous smart windows [21, 22]. On the other hand, when the MIT layer is on the opposite pane (S_2 configuration) the incoming net flux becomes more important, the temperature of this pane being increased by the greenhouse effect. Notice that the presence of a convective exchange between the environment and the window reduces its equilibrium temperature.

Beside the thermal characteristics of the window we show in Fig.4(d) the transmittance

$$T(\omega) = \int_0^{\pi/2} (t_s(\omega, \theta) + t_p(\omega, \theta)) \cos \theta \sin \theta d\theta \quad (4)$$

of the smart window in the visible range for both phases of thermochromic material. Here t_s (resp. t_p) denotes the directionnal spectral transmission of the window under an incident angle θ (with respect to the normal, see Fig.1) in s (resp. p) polarization. Notice that this transmittance depends weakly, in the visible, on the crystallographic state of VO_2 film, the main changes taking place mainly in the infrared. Although relatively small, this transmittance ($\sim 35\%$) over 75% of spectrum is comparable with the usual double glazing SiO_2 - SiO_2 . Moreover, this value could be significantly improved using a nanostructured active layer without significantly affecting its properties in the infrared as discussed in Ref. [21–24].

In conclusion we have introduced a smart window based on a double glazing made with a SiO_2 - VO_2 bilayer which is autonomously thermally and optically regulated by greenhouse effect. This system overcomes the primary weaknesses of thermochromic and electrochromic smart windows. Beyond its application in the development of smart windows for more sustainable buildings, the passive insulation mechanism introduced in the present work could find broader applications in the development of self-regulated insulating materials for complex systems.

Acknowledgments

This research was supported by the French Agence Nationale de la Recherche (ANR), under grant ANR-19-CE08-0034 (PassiveHEAT). P. B.-A. acknowledges discussions with E. Blandre and A. Losquin.

Data availability

The data that support the findings of this study are available from the corresponding authors upon reasonable request.

-
- * Electronic address: pba@institutoptique.fr
- [1] T. Ramesh, R. Prakash, K. K. Shukla, Life cycle energy analysis of buildings: An overview. *Energy Build.* **42**, 1592-1600 (2010).
- [2] H. Kim et al., *ACS Nano* **7**, 5769-5776 (2013).
- [3] J. Zheng et al., *Nano Energy* **11**, 136-145 (2015).
- [4] T. Chang et al., *Nano Energy* **44**, 256-264 (2018).
- [5] P. Ben-Abdallah and S. A. Biehs, *Appl. Phys. Lett.*, **103** (19), (2013).
- [6] P. Ben-Abdallah, H. Benisty and M. Besbes, *J. Appl. Phys.*, **116** (3) (2014).
- [7] P. Ben-Abdallah and S.-A. Biehs, *Phys. Rev. Lett.* **112**, 044301 (2014).
- [8] A. Fiorino et al., *ACS NANO* **12** (6) , 5774-5779 (2018).
- [9] D. G. Baranov et al., *Nature Materials*, **18**, 920 (2019).
- [10] V. Kubytskyi, S.-A. Biehs and P. Ben-Abdallah, *Phys. Rev. Lett.* **113**, 074301 (2014).
- [11] P. Ben-Abdallah and S.-A. Biehs, *Phys. Rev. B* **94**, 241401(R) (2016).
- [12] A. Cannavale et al., *Energies*, **13**, 1449 (2020).
- [13] S. Chen et al., *Sci. Adv.* **2019**;5: eaav6815 (2019).
- [14] M. M. Qazilbash, M. Brehm, B. G. Chae, P.-C. Ho, G. O. Andreev, B. J. Kim, S. J. Yun, A. V. Balatsky, M. B. Maple, F. Keilmann, H. T. Kim, and D. N. Basov, *Science*, **318**, 5857, 1750-1753 (2007).
- [15] A. S. Barker, H. W. Verleur, and H. J. Guggenheim, *Phys. Rev. Lett.* **17**, 1286 (1966).
- [16] H. W. Verleur, A. S. Barker and C. N. Berglund, *Phys. Rev.* **172**, 788 (1968)
- [17] *Handbook of Optical Constants of Solids*, edited by E. Palik (Academic Press, New York, 1998).
- [18] S.-A. Biehs, R. Messina, P.S. Venkataram, A. W. Rodriguez, J. C. Cuevas and P. Ben-Abdallah, *Rev. Mod. Phys.*, **93**, 025009 (2021).
- [19] I. Latella, P. Ben-Abdallah, S.-A. Biehs, M. Antezza and R. Messina, *Phys. Rev. B* **95**, 205404 (2017).
- [20] NREL (2004), Reference Solar Spectral Irradiance: Air Mass 1.5, (rredc.nrel.gov/solar/spectra/am1.5).
- [21] M. Feng et al., *J. Mater. Sci.*, **55**, 8444-8463 (2020).
- [22] Y. Cui et al., *Joule*, **2**, 9, 1707-1746 (2018).
- [23] A. Taylor et al., *Opt. Exp.* **21**, 18, A750-A764 (2013)
- [24] S. Liu et al., *Sci. Rep.*,**10**:11376 (2020).